

# Cognitive Radio for Asymmetric Cellular Downlink with Multi-User MIMO

Omer Gokalp Serbetci, *Student Member, IEEE*, Lei Chu, *Senior Member, IEEE* and Andreas F. Molisch, *Fellow, IEEE*

Ming Hsieh Department of Electrical and Computer Engineering, University of Southern California, Los Angeles, USA

{serbetci, lc\_285, molisch}@usc.edu

**Abstract**—Cognitive radio (CR) is an important technique for improving spectral efficiency, letting a secondary system operate in a wireless spectrum when the primary system does not make use of it. While it has been widely explored over the past 25 years, many common assumptions are not aligned with the realities of 5G networks. In this paper, we consider the CR problem for the following setup: (i) infrastructure-based systems, where downlink transmissions might occur to Receivers (Rx) whose positions are not, or not exactly, known; (ii) multi-beam antennas at both primary and secondary base stations. We formulate a detailed protocol to determine when secondary transmissions into different beam directions can interfere with primary users at *potential* locations and create probability-based interference rules. We then analyze the “catastrophic interference” probability and the “missed transmission opportunity” probability, as well as the achievable throughput, as a function of the transmit powers of the primary and secondary base stations and the sensing window of the secondary base station. Results can serve to more realistically assess the spectral efficiency gains in 5G infrastructure-based cognitive systems.

**Index Terms**—Spectrum Sensing, Cognitive Radio

## I. INTRODUCTION

As the demand for wireless services increases, new adaptive methods for utilizing the wireless spectrum become necessary. Traditionally, spectrum has been assigned to specific entities, such as network operators or defense agencies. However, newly released bands are often made available with the stipulation that (temporarily) unused frequency resources can be exploited by users who do not belong to the nominal “owner” of the spectrum. In particular, the recent establishment of the Citizen Broadband Radio Service by the Federal Communication Commission, in which new services such as 5G are allowed to operate in certain mid-band (3.5 GHz) bands with legacy users has added significant relevance to this topic both from the military and civilian/economic point of view [1].

The trend toward adaptive spectrum usage began more than 20 years ago under the name of Cognitive Radio (CR) and has seen a surge of interest, e.g., [2], [3]. A cognitive radio system is characterized by the presence of a *primary* system, which includes infrastructure and user nodes, as well as a secondary system. The key requirement is that the activities of the secondary system do not (or only within specified limits) degrade the performance of the primary system. To ensure this, the secondary system must monitor the spectrum occupancy of the primary system and decide whether or not to transmit in order to avoid interference [4, Chap. 26].

Although there are thousands of papers on CR, the current work focuses on a scenario that has received comparatively little attention despite being practically important: *CR in an infrastructure-based system using directional transmissions, where downlink transmissions may occur to User Equipments (UEs) whose locations are unknown or only partially known*. Conventional CR approaches often assume that (i) nodes transmit in all directions and (ii) that primary nodes operate in a manner that allows the secondary system to infer the location of, or the propagation channel to, the potential victim (primary) Rx, see also Sec. III. Neither of these assumptions typically holds in a 5G system. Regarding (i), the use of multiple antennas (and hence beamforming capabilities in various directions) is a mandatory part of the 3GPP NR standard [5]. Regarding (ii), identifying the location (or channel) of the currently *actively receiving* Primary User (PU), i.e., the victim Rx, can be difficult or even impossible. In the 5G standard, there are generally no uplink signals (i.e., from the PU to the Primary Base Station (PBS)) that *precede* downlink transmission; see Sec. IV for details.

To overcome these limitations, this paper presents a detailed model for directional sensing and decision-making in the *downlink* of an *infrastructure-based* system (e.g., cellular 5G), where both the PBS and Secondary Base Station (SBS) use multi-beam (sectorized) antennas. While the channels between the PBS and all *potential* PU locations are assumed to be known (e.g., through training and feedback over time), the identities and locations of the *currently active* PUs (i.e., those receiving downlink transmissions) are unknown. The SBS must therefore perform three tasks: (i) learn - through a process described in Sec. IV - whether transmission from each SBS beam creates “significant” interference, defined via the Signal-to-interference-plus-noise Ratio (SINR), to each *potential* PU location; (ii) sense, in each of its beams, the transmission from the PBS to determine which PBS beams are currently active - a task that can be formulated as a multi-binary hypothesis testing problem; and (iii) based on this information, determine which SBS beams are permitted to transmit without exceeding a specified statistical interference threshold at the PUs.

The main contributions of this work are thus

- Formulation of the cognitive problem for the downlink in the infrastructure-based primary and secondary system, undetectable location/channels of the PUs, and multi-

- beam PBS and SBS.
- Designing a novel downlink transmission decision rule for the SBS.
- Performing simulations based on realistic (ray-tracing) channel configurations, demonstrating the performance.

## II. RELATED WORK

Since Spectrum Sensing (SS) and CR are well-established research areas, numerous aspects have been explored over the years, including sensing approaches and transmission decision criteria and algorithms, based on a variety of system models, see [2], [3] and references therein.

Most prior works assume omnidirectional antennas and formulate sensing as a binary hypothesis test over the entire region. Directional setups, when explored, often focus on single-source localization [6] or transmitter detection using switched-beam antennas in distributed networks [7]. Cooperative sensing has been studied in both distributed [8] and centralized [9] frameworks. Still, these typically assume full-duplex operation or synchronized Tx/Rx cycles that permit estimation of channels from secondary TXs to currently active primary Rx — assumptions that do not hold in our system model. Additional studies explore directional sensing via stochastic geometry [10], [11], capacity analysis for directional Secondary User (SU) networks [12], and beam selection strategies to improve detection performance [9].

More related to our case is [13], which bypasses explicit sensing and directly allocates SBS power based on sensing inputs, without modeling the PBS. Key differences include: (i) lack of a communication model; (ii) knowledge of instantaneous PU activity via dedicated sensors, unlike our use of PBS downlink signals; (iii) interpolation of sparse data versus our learned channel estimates; and (iv) a strict zero-interference constraint, while we allow controlled interference.

The most comparable work is [14], which tackles the beam detection subtask but relies on supervised learning with labels from the primary system to the secondary system. In contrast, we assume that such collaboration is not allowed/feasible, as it requires changes in the primary system; rather, we aim to detect active PBS beams solely from SBS observations and select interference-aware SBS beams to serve SUs. Thus, our work fundamentally differs in system modeling and operational assumptions.

## III. SYSTEM MODEL

This section outlines the operation of the PBS and SBS, along with the associated signal and channel models. The PBS operates with a common slotted time structure consisting of  $I$  equal-length intervals. During each interval  $i \in \mathcal{I} \triangleq \{1, 2, \dots, I\}$ , spanning  $T_{i-1} \leq t \leq T_i$ , the PBS transmits packets to the PUs. We define the set of all possible UE locations (either PUs or SUs) within the region of interest as  $\mathcal{S} \triangleq \{z_1, z_2, \dots, z_U\}$ , where  $z_u \in \mathbb{R}^2$  denotes the

coordinates of UE  $u \in \mathcal{U}$ . The set of UE indices is denoted by  $\mathcal{U} \triangleq \{1, 2, \dots, U\}$ .

### A. Multi-Beam Configuration at the Base Stations

We assume that the PBS and SBS have  $B_{\text{PBS}}$  and  $B_{\text{SBS}}$  beams, respectively, dividing the azimuth plane into (potentially non-uniform) sectors. Each beam, indexed  $k$ , of the PBSs might be active (ON) or inactive (OFF) during interval  $i$ , as indicated by the  $b_{i,k}^{\text{PBS}} \in \{0, 1\}$ ; the set of activity indicators in slot  $i$  is  $\mathcal{B}_i^{\text{PBS}} \in \{0, 1\}^{B_{\text{PBS}}}$ .

The SBS adopts the same basic time structure as the PBS, but each interval  $i$  is divided into two sub-intervals: sensing ( $T_{i-1} \leq t \leq T_i^{\text{sensing}}$ ) and transmission ( $T_i^{\text{sensing}} \leq t \leq T_i$ ). During the  $i^{\text{th}}$  sensing phase, the SBS collects  $N$  samples indexed by  $n \in \{1, \dots, N\}$  in each beam, thereby obtaining observations of the PBS signals. We assume that the SBS can obtain samples on all its beams simultaneously (i.e., no beam sweeping is required). Based on these observations, the SBS determines the set of beams it uses for transmission in the  $i^{\text{th}}$  interval, similarly represented as  $\mathcal{B}_i^{\text{SBS}} = \{b_{i,l}^{\text{SBS}}\}_{l=1}^{B_{\text{SBS}}}$ . The SBS knows  $B_{\text{PBS}}$  and the  $T_i$ ; for notational simplicity, we further assume that both the primary and secondary systems operate over the same known bandwidth  $BW$ , consisting of  $F$  equally spaced frequencies  $\mathcal{F} \triangleq \{f_j\}_{j=1}^F$ . All these parameters can be obtained from standards or equipment specifications. However, we stress that (i) the SBS does not know with which PUs the PBS communicates, and (ii) it must infer from its sensing results which PBS sectors are active. Fig. (1) illustrates an example configuration, showing beam orientations for both PBS and SBS, along with example PUs and SUs in the environment.

The  $n^{\text{th}}$  signal sample received in the  $l^{\text{th}}$  beam of the SBS, corresponding to the transmission from the PBS on frequency  $f_j$  during the  $i^{\text{th}}$  sensing interval, is denoted by  $r_{i,j,l,n}^{\text{SBS}}$  is

$$r_{i,j,l,n}^{\text{SBS}} = \sum_{k=1}^{B_{\text{PBS}}} b_{i,k}^{\text{PBS}} \cdot h_{j,k,l}^{\text{PBS} \rightarrow \text{SBS}} \cdot s_{i,j,k,n}^{\text{PBS}} + w_{i,j,l,n} . \quad (1)$$

The signal transmitted on the  $k^{\text{th}}$  beam at frequency  $f_j$  is denoted as  $s_{i,j,k,n}^{\text{PBS}}$  and is modeled as Gaussian random variable  $\sim \mathcal{CN}(0, \sigma_{\text{PBS}}^2)$  since both the payload data and the modulation format are unknown to the SBS. The complex channel transfer function at frequency  $f_j$  from the  $k^{\text{th}}$  PBS beam to the  $l^{\text{th}}$  SBS beam is denoted as  $h_{j,k,l}^{\text{PBS} \rightarrow \text{SBS}} \in \mathbb{C}$  and assumed to be constant over the duration of a packet. Each received sample is also corrupted by additive complex Gaussian noise  $w_{i,j,l,n} \sim \mathcal{CN}(0, \sigma_{\text{noise}}^2)$ , where noise power is assumed constant across frequency, beam, and time.

The complex channel gain can be described as the sum of  $M$  weighted contributions of the Multipath Components (MPCs)

$$h_{j,k,l}^{\text{PBS} \rightarrow \text{SBS}} = \sum_{m=1}^M |\alpha_m| e^{i\phi_m} e^{-i2\pi\tau_m f_j} \beta_k(\Omega_m) \beta_l(\Psi_m) \quad (2)$$

Here, the complex gain, phase, delay, direction of departure (DoD), and direction of arrival (DoA) of the  $m^{\text{th}}$  MPC are denoted by  $\alpha_m$ ,  $\phi_m$ ,  $\tau_m$ ,  $\Omega_m$ , and  $\Psi_m$ , respectively. Moreover, the antenna pattern corresponding to the  $k^{\text{th}}$  beam of the PBS is represented by

$$\beta_k(\Omega_m) = \sum_{n=1}^{B_{\text{PBS}}} e^{jn\pi(\cos \Omega_m - \cos \Omega_k)}, \quad (3)$$

where  $\Omega_k$  is the steering angle for sector  $k$ . The pattern  $\beta_l(\Psi_m)$  for the  $l^{\text{th}}$  beam of the SBS is defined similarly.

We partition the location set  $\mathcal{S}$  into mutually exclusive subsets corresponding to the PBS beam sectors as  $\mathcal{S} = \bigcup_{k=1}^{B_{\text{PBS}}} \mathcal{S}_k^{\text{PBS}}$ , where  $\mathcal{S}_k^{\text{PBS}} \cap \mathcal{S}_l^{\text{PBS}} = \emptyset$  for all  $k \neq l$ . The corresponding PU index set is similarly partitioned as  $\mathcal{U} = \bigcup_{k=1}^{B_{\text{PBS}}} \mathcal{U}_k^{\text{PBS}}$ . The association between a UE and a beam of the Base Station (BS) is based on the small-scale-averaged path gain. In line-of-sight (LOS) scenarios, this association may admit a geometric interpretation, though this is not strictly required. The beam associated with the UE located at  $\mathbf{z}_u$  with respect to the PBS is defined as

$$c_u^{\text{PBS}} \triangleq \arg \max_k \frac{1}{F} \sum_{j=1}^F |h_{j,k,u}^{\text{BS} \rightarrow \text{UE}}|^2. \quad (4)$$

The corresponding beam associations with respect to the PBS are denoted by  $c_u^{\text{PBS}}$ . Accordingly,  $c_u^{\text{PU}} = k$  for all  $u \in \mathcal{U}_k^{\text{PBS}}$ .

For ease of notation, we discuss the case of a single PBS. Generalization to multiple PBSs is straightforward as it generates a larger set of PBS sectors (and similarly for SBS), and the same data collection and transmission decision rules can be applied; however, it increases the numerical complexity of obtaining solutions.

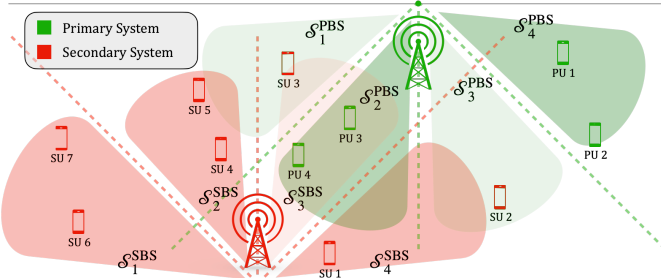


Figure 1: Illustration of primary and secondary beams with scattered PUs and SUs; inactive beams are shown with light shading.

### B. Interference Estimate in Asymmetrical Downlink

To assess potential performance degradation at the PUs, we model the received signals as a function of the SBS operation. During  $T_i^{\text{sensing}} \leq t \leq T_i$ , the SBS uses the set of beams  $\mathcal{B}_i^{\text{SBS}}$  (selection of this set is discussed in Sec. IV). The received signal at the PU is modeled as the sum of the signals from the active PBS and SBS beams, each weighted by its respective channel. The received sample is further corrupted by additive

complex Gaussian noise. The signal transmitted by the SBS, similar to that of the PBS, is modeled as a zero-mean complex Gaussian random variable with power  $\sigma_{\text{SBS}}^2$ . The channel at  $f_j$  between the  $k^{\text{th}}$  beam of a base station and a UE located at position  $\mathbf{z}_u$  is

$$h_{j,k,u}^{\text{BS} \rightarrow \text{UE}} = \sum_{m=1}^M |\alpha_{u,m}| e^{i\varphi_{u,m}} e^{-i2\pi\tau_{u,m}f_j} \beta_k^{\text{BS}}(\Omega_{u,m}). \quad (5)$$

The definitions of the MPCs are analogous in Eq. (2). The only difference is the absence of the antenna gain term corresponding to the direction of arrival, since the UEs are assumed to have omnidirectional antennas. Associations between a PU and an SBS sector are denoted by  $c_u^{\text{SBS}}$ , analogously to the association between PU and a PBS sector. The SINR for PU  $u$  at location  $\mathbf{z}_u$  during interval  $i$  is defined as  $\text{SINR}_{i,u} \triangleq \frac{P_{i,u}^{\text{signal}}}{P_{i,u}^{\text{int}} + P_{i,u}^{\text{noise}}}$ . The received signal power from the associated PBS beam is given by

$$P_{i,u}^{\text{signal}} \triangleq b_{i,c_u^{\text{PBS}}}^{\text{PBS}} \sigma_{\text{PBS}}^2 \frac{1}{F} \sum_{j=1}^F |h_{j,c_u^{\text{PBS}},u}^{\text{PBS} \rightarrow \text{PU}}|^2. \quad (6)$$

The total interference power is decomposed as  $P_{i,u}^{\text{int}} \triangleq P_{i,u}^{\text{Pint}} + P_{i,u}^{\text{Sint}}$ , where  $P_{i,u}^{\text{Pint}}$  accounts for inter-beam interference from the PBS

$$P_{i,u}^{\text{Pint}} \triangleq \sigma_{\text{PBS}}^2 \sum_{\substack{k=1 \\ k \neq c_u^{\text{PBS}}}}^{B_{\text{PBS}}} b_{i,k}^{\text{PBS}} \frac{1}{F} \sum_{j=1}^F |h_{j,k,u}^{\text{PBS} \rightarrow \text{PU}}|^2 \quad (7)$$

while the interference from SBS transmissions is

$$P_{i,u}^{\text{Sint}} \triangleq \sigma_{\text{SBS}}^2 \sum_{l=1}^{B_{\text{SBS}}} b_{i,l}^{\text{SBS}} \frac{1}{F} \sum_{j=1}^F |h_{j,l,u}^{\text{SBS} \rightarrow \text{PU}}|^2. \quad (8)$$

### C. Problem Formulation

Traditional CR assumes that the channels between primary Rx and primary and secondary Transmitters (Tx) (or Tx sectors) are known. Sensing whether a particular primary Tx (sector) is active, which is a binary detection problem, then allows us to determine whether activating a particular secondary Tx is permissible. The key difference in the setup we consider is that the specific set of actively receiving PUs in the  $i$ -th timeslot is unknown. This is motivated by the structure of 5G transmissions as discussed in more detail in Sec. IV-A. The beam selection process at the SBS is thus based solely on (i) the estimated set of currently active PBS beams,  $\hat{\mathcal{B}}_i^{\text{PBS}}$ , and (ii) a probabilistic constraint requiring that, on average, the fraction of PUs experiencing significant interference remains below a predefined threshold.

Formally, for each interval  $i$  and sector  $k$ , we require that the probability of a randomly selected active PU  $u \sim \mathcal{P}_k^{\text{PU}}$  experiencing SINR below a minimum threshold  $\theta$  satisfies

$$\Pr_{u \sim \mathcal{P}_k^{\text{PU}}}(\{ \text{SINR}_{i,u} < \theta \}) = \sum_{u_{\text{act}} \in \mathcal{U}_k} \Pr(u = u_{\text{active}}) \quad (9)$$

$$\times \Pr(\{ \text{SINR}_{i,u} < \theta \} \mid u = u_{\text{active}}) < V.$$

Here,  $\theta$  represents the minimum SINR required for reliable PU operation, and  $V$  denotes the maximum permissible fraction of locations where the SINR may fall below this threshold due to SBS transmissions.<sup>1</sup>  $\Pr(u = u_{\text{active}})$  is the spatial probability distribution of the PUs. We assume in the following that the SBS has no knowledge at all about the spatial distribution and thus use a uniform distribution  $\Pr(u = u_{\text{active}}) = 1/|\mathcal{U}_k|$ .

More detailed distributions can, e.g., be learned over time by the SBS through uplink transmissions and their association with location-specific channel state information. It can also incorporate probabilistic information about the set of PUs that might be intended as Rx in a given timeslot, e.g., based on traffic patterns and uplink/downlink correlations. These aspects will be explored more in our future work.

Finally, the optimization aims to serve, with a given (or estimated) set of active PBS sectors, the maximum number of SUs without violating the PU interference constraint. We furthermore assume that the SBS throughput is maximized by maximizing the number of SBS beams that are active:

$$\max_{b_{i,l}^{\text{SBS}}} \sum_{l=1}^{B_{\text{SBS}}} b_{i,l}^{\text{SBS}} \quad \text{s.t. (9), } \forall i \in \mathcal{I}. \quad (10)$$

#### IV. ALGORITHM

We now come to the core of this paper, namely the algorithm for determining which SBS sectors can transmit in which timeslots. This algorithm proceeds in two phases: an offline phase in which the SBS learns the UE-PBS and UE-SBS channels for each UE location, and an online phase, in which the SBS decides, for each timeslot, which SBS beams may transmit. *Notably, in both phases, we do not utilize any information about the active PUs, including their locations or channel states.*

##### A. Offline Phase

The equations in Sec. III assume that the channels between the PU and both the PBS and the SBS are known to the SBS—an assumption commonly made in the CR literature. However, in typical 5G cellular systems, this assumption does not hold due to the structure of uplink and downlink transmissions. A 5G BS might be connected to dozens or hundreds of UEs, and it is impossible for somebody without access to the scheduler of the BS to know which UE will be scheduled

<sup>1</sup>This formulation assumes that, in the absence of SBS transmissions, all PUs meet the SINR requirement. The PBS scheduler will typically ensure that this condition is fulfilled.

in the next downlink transmission slot. In particular, downlink transmissions are not necessarily preceded by any uplink activity [5], [4, Chap. 32]. While acknowledgment (ACK) packets are typically sent on the uplink *after* a downlink transmission, this feedback arrives too late to be useful for CR applications.<sup>2</sup> Furthermore, in multicast scenarios, uplink transmissions may be absent altogether, rendering it even more difficult to identify the active PU locations or channel conditions.

We propose, however, that what *can* be achieved is knowledge of the PBS-PU and SBS-PU channels (more precisely, between each sector of PBS and PU, and similarly for the SBS) for a given UE location. To this end, we introduce the following protocol:

- 1) A SU observes the transmission from the PBS and records its time of observation, primary signal characteristics (e.g., occupied frequency), as well as its own location.
- 2) Within a short time (e.g., at the next secondary uplink transmission opportunity), the SU transmits this information to the SBS. This transmission provides the SBS not only with the observations made by the SU, but also enables it to measure the channel from the SU location to the SBS, which—due to channel reciprocity<sup>3</sup>—is also the channel from the SBS to the UE. Furthermore, the SBS continuously monitors transmissions from the PBS and records the corresponding information along with timestamps.<sup>4</sup>
- 3) The SBS thus obtains knowledge of the PBS transmission status, the UE’s location, the PBS - UE channel (pathloss), and the SBS - UE channel. While the sensing UE is an SU, the channel and the received power from a BS to a UE are independent of whether the UE is a PU or an SU!

These channels need to be determined at every UE location<sup>5</sup> within the cell; thus the observing SUs have to cover all locations within the cell and observe any combinations of PBS beam transmission. This leads to a long required duration for the learning process; the corresponding channel between a UE in a particular location and a BS is assumed to be time invariant during the learning process, which is approximately fulfilled since dominant scatterers like buildings are static. Residual variations, e.g., due to moving scatterers like cars, are neglected here because they typically have a small radar

<sup>2</sup>Even in cases of repeated packet transmissions, such as during streaming—where an ACK packet could suggest future packets might be sent to the same UE—these ACKs may occur at time-frequency resources with no discernible relation (from the SBS perspective) to the preceding downlink signal. Moreover, they may be indistinguishable from UE-initiated transmissions, making them ineffective for inferring the location or channel of the PU.

<sup>3</sup>In frequency division duplex systems, the small-scale-averaged characteristics are reciprocal, while in time division duplex systems, even complex channel gains might be reciprocal.

<sup>4</sup>Note that the SBS does not require knowledge of the PBS geometry or its beam patterns; it can describe active PBS beams and infer user associations solely based on the observed channel states between the PBS and the SBS.

<sup>5</sup>Since we only need the small-scale averaged (SSA) channel characteristics, it is sufficient to measure at one location within a “stationarity” region of the channel, which is typically on the order of a few tens of meters in outdoor environments, [4, Chapter 7]

cross section and only introduce minor channel variations; their impact will be considered in future work.

The output of the offline phase are thus the channels for different PBS beam combinations,  $\mathcal{B} \triangleq \{b_k\}_{k=1}^{B_{\text{PBS}}} \in \{0, 1\}^{B_{\text{PBS}}}$ , and the corresponding expected energy label vector  $g(\mathcal{B}) \in \mathbb{R}^{B_{\text{SBS}}}$  by averaging over many frames. Assuming Gaussianity of the noise-induced variations, the  $l^{\text{th}}$  entry of  $g(\mathcal{B})$  is given by

$$g_l(\mathcal{B}) = \sum_{k=1}^{B_{\text{PBS}}} \sum_{j=1}^F b_k^{\text{PBS}} \sigma_{\text{PBS}}^2 |h_{j,k,l}^{\text{PBS} \rightarrow \text{SBS}}|^2 + \sigma_{\text{noise}}^2. \quad (11)$$

This allows computation of an SINR table for each location  $\mathbf{z}_u$ ,  $\text{SINR}_u$  with respect to  $\mathcal{B}^{\text{PBS}}$  and  $\mathcal{B}^{\text{SBS}}$ , where each entry corresponds to a unique combination of PBS and SBS beam activity. The index  $i$  is omitted, as the table remains the same in all sensing intervals and does not depend on  $i$ .

### B. Online Phase

In each time interval  $i$  the SBS needs to (i) estimate, at the end of the sensing phase, the active PBS beams  $\hat{\mathcal{B}}_i^{\text{PBS}}$  based on the  $N$  collected samples, and (ii) select a subset of SBS beams to transmit packets to the SUs, ensuring that the service quality of the PUs  $\text{SINR}_{i,u}$  for the given  $b_{i,k}^{\text{PBS}}$  and the chosen  $b_{i,l}^{\text{SBS}}$  is not excessively degraded as per (9).

#### 1) Detection of PBS Beams

During the offline phase, we assume that the SBS can perfectly associate PBS activity with the received signals, owing to the static nature of the environment and the extended measurement duration. In contrast, during the online phase, the SBS must detect PBS activity based on a limited number of sensing samples, which may introduce detection inaccuracies. To detect the active (ON) beams of the PBS, we employ a simple energy detector based on a maximum-likelihood (ML) rule. Specifically, given the observed energies across SBS beams, we select the most likely configuration among the  $2^{B_{\text{PBS}}}$  possible PBS beam combinations. The energy measured during sensing interval  $i$  on beam  $l$  of the SBS is defined as

$$v_{i,l}^{\text{SBS}} \triangleq \frac{1}{N} \sum_{n=1}^N \sum_{j=1}^F |r_{i,j,n,l}^{\text{SBS}}|^2. \quad (12)$$

We then stack the energy across all beams into a feature vector  $\mathbf{x}_i \triangleq [v_{i,1}^{\text{SBS}}, \dots, v_{i,B_{\text{SBS}}}^{\text{SBS}}]$ , where  $\mathbf{x}_i \in \mathbb{R}^{B_{\text{SBS}}}$ . Given the observed energy  $\mathbf{x}_i$ , we estimate the active PBS beams via maximum-likelihood detection as  $\hat{\mathcal{B}}_i^{\text{PBS}} = \arg \min_{\mathcal{B}} \|\mathbf{x}_i - g(\mathcal{B})\|^2$ .

#### 2) SBS Transmission Decision

Based on the identified active transmission beams of the PBS, we assess whether, and in which directions, the SBS is permitted to transmit without catastrophic interference to actively receiving PUs; i.e., solve (10). Taking the SINR table entries for the estimated  $\hat{\mathcal{B}}_i^{\text{PBS}}$ , we can find  $\mathcal{B}_i^{\text{SBS}} = \arg \max_{\mathcal{B}} \sum_{l=1}^{B_{\text{SBS}}} b_l$  subject to the constraint that the average SINR for PUs in  $\mathcal{U}_k$  remains above a given threshold under the

selected configuration, as formalized in Eq. (9). In other words, we search for all the SBS beam combinations that do not lead to catastrophic interference, i.e., ensure that the increase in PUs whose SINR threshold exceeds  $\theta$  increases beyond a threshold  $V$ . We note that besides this constraint, other criteria, like maximum reduction of average capacity or outage capacity, could be imposed. Furthermore, the maximization of the number of secondary beams could be replaced by maximizing throughput for the scheduled SUs (since the SBS knows the channels to the SUs) could be employed. While all these results give slightly different optimization results, the protocols and algorithmic frameworks remain unchanged.

## V. NUMERICAL EVALUATION

**Dataset.** We evaluate our algorithm by using ray tracing to obtain realistic propagation channels; we use the *Wireless InSite* tool for generating MPCs parameters (see (2)) between the PBS and SBS, as well as between each (single-antenna) UE and the BSs. Simulations shown in the following are done on the USC campus near the TCC building, at a carrier frequency of 2.5 GHz, bandwidth of 1 MHz, and using beamforming via a spatial Fourier transformation of a uniform linear array as commonly used in 5G [4]. Further simulation details are omitted due to space constraints.

The PBS does not perform power control; its transmit power is chosen such that it provides a minimum of 3 dB Signal-to-noise Ratio (SNR) to each PU in the environment. In our setup, we found  $\sigma_{\text{PBS}}^2 = 5 \text{ dBm}$ . The SBS is not assumed to have power control capability, but its transmit power  $\sigma_{\text{SBS}}^2$  is a system parameter we vary in the subsequent simulations to study its impact. We further assume that the beamforming gains of both PBS and SBS are absorbed into the transmit powers; thus,  $\sigma_{\text{PBS}}^2$  and  $\sigma_{\text{SBS}}^2$  represent the equivalent isotropically radiated power (EIRP). The activity of each PBS beam  $b_{i,k}$  is modeled as an i.i.d. Bernoulli random variable where  $b_{i,k} = 1$  with probability 1/2.

**Baselines.** *Multi-Detection Binary Access*, which uses the same hardware setup with directional antennas. The SBS predicts the individual beam activity,  $\hat{\mathcal{B}}_i^{\text{PBS}}$ , and the transmission is binary—SBS either transmits all of the beams (if the SINR constraints are satisfied) or remains silent. *Binary-Detection Binary Access*, a conventional SS method, detects only the presence of any PBS activity without directionality. It transmits omnidirectionally if no PBS beam is active (unlike the former, which can still transmit even if there is PBS activity, as long as the SINR constraints are satisfied); otherwise, it remains silent. For consistency, the transmission power levels are kept identical to those in the directional case.

### A. Results

We evaluate our system using three criteria defined as follows.

**Probability of Missed Opportunity (PMO).** This metric quantifies the percentage of SBS beams that satisfy the SINR

constraints and could have been used for transmission, but were not selected, primarily due to misdetection of active PBS beams. We define the total number of admissible transmissions as  $B_{\text{mo}} \triangleq \sum_{i=1}^I \sum_{l=1}^{B_{\text{SBS}}} b_{i,l}^{\text{SBS, GT}}$ , where GT denotes the ground truth obtained under the assumption of perfect knowledge of the PBS beam activity in each interval. Accordingly, the PMO is defined as

$$C_{\text{mo}} \triangleq \frac{1}{B_{\text{mo}}} \sum_{i=1}^I \sum_{l=1}^{B_{\text{SBS}}} 1\{b_{i,l}^{\text{SBS, GT}} = 1\} 1\{b_{i,l}^{\text{SBS}} = 0\}. \quad (13)$$

**Probability of Catastrophic Interference (PCI).** The main constraint for the secondary system is the potential catastrophic interference that PUs experience once the secondary system is active.  $C_{\text{int}}$  describes the percentage of the PUs that had severe interference after the SBS transmission, where the total number of beams active in the environment is defined as  $B_{\text{int}} \triangleq \sum_{i=1}^I \sum_{l=1}^{B_{\text{PBS}}} b_{i,k}^{\text{PBS}}$ . Then, the PCI is defined as

$$C_{\text{int}} \triangleq \frac{1}{B_{\text{int}}} \sum_{i=1}^I \sum_{k=1}^{B_{\text{PBS}}} 1\left\{ \left( \frac{b_{i,k}}{|\mathcal{U}_k|} \sum_{u \in \mathcal{U}_k} 1\{\text{SINR}_{i,u} < \theta\} \right) > V \right\}. \quad (14)$$

**Throughput.** Since the main objective of all CR efforts is to serve the secondary users, we assess the performance of the proposed scheme in terms of the throughput of the secondary system, which is evaluated as

$$C_{\text{thru}} \triangleq \frac{1}{I} \sum_{i=1}^I \sum_{u=1}^U \frac{1\{\text{SINR}_{i,u}^{\text{SBS}} > \theta\}}{U}. \quad (15)$$

Secondly, the  $\text{SINR}_{i,u}^{\text{SBS}}$  is computed based on the SBS beam configuration, analogous to the SINR calculation for the PBS, but with the PBS and SBS roles interchanged, as the evaluation is for the SUs.

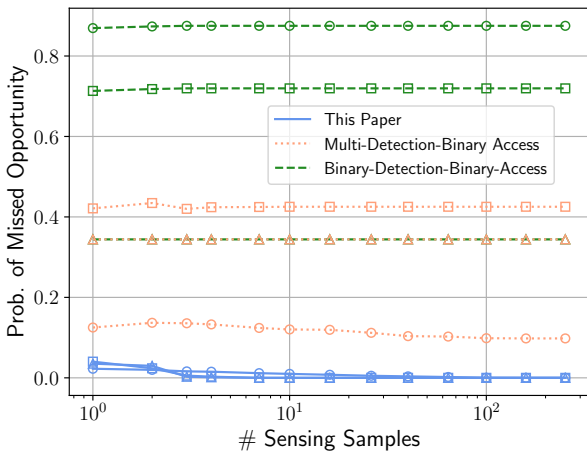


Figure 2: PMO Comparison for different  $\sigma_{\text{SBS}}^2 / \sigma_{\text{PBS}}^2$  as  $\circ$ : -20 dB,  $\square$ : -5 dB,  $\triangle$ : 5 dB. MDBA and BDBA for 5 dB overlap.

In Fig. (2), we compare the PMO as a function of the number of sensing samples that SBS gathered and show results for different SBS powers. In the case of perfect estimation of the PBS beam state, our method, by definition, incurs no missed transmission opportunities; this is achieved after 100 samples. However, when the PBS beam state is misestimated, the SBS may refrain from transmitting in certain directions due to erroneously predicted interference. The binary-detection baseline, which waits for complete PBS silence, misses the most transmission opportunities. Although the multi-detection baseline senses directionally, it still transmits only when all directions are deemed safe, leading to more missed opportunities than our method. We also see that while the PMO for our method depends mostly on the number of sensing samples, and thus on the accuracy of the PBS beam identification, the PMO for the other methods is dominated by the ratio of SBS to PBS power. This can be explained by the increased probability that even secondary beams with small power coupling into PBS beams create significant interference, which, according to the principle of the baseline, prevents *all* transmissions from the SBS and thus increases the PMO.

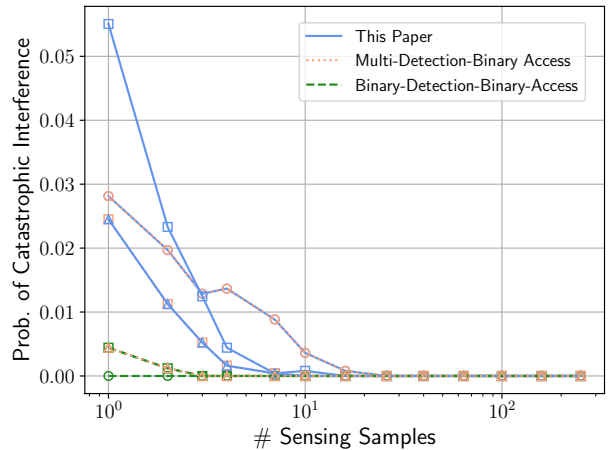


Figure 3: PCI Comparison, for different  $\sigma_{\text{SBS}}^2 / \sigma_{\text{PBS}}^2$  as  $\circ$ : -20 dB,  $\square$ : -5 dB,  $\triangle$ : 5 dB. Our method and MDBA for -20 dB overlap. MDBA (5 dB) and BDBA (-5 dB) overlap. Our method (5 dB) and MDBA (-5 dB) overlap.

A similar study is done for the PCI in Fig. (3). Note, however, that absence of CI does *not* mean that there are zero PUs impacted by interference, just that the percentage of catastrophically interfered PUs in one beam remains below the threshold  $V$ . Note that for the low number of sensing samples, our algorithm may lead to higher PCI, since it exploits *all* apparent transmission opportunities (even when they are just a consequence of the erroneous PBS beam activity). However, the use of a longer sensing window (100 samples) essentially eliminates this problem. While this reduces the available transmission time for the secondary payload, this is more than compensated by the increased probability of transmission as shown in Fig. (4).

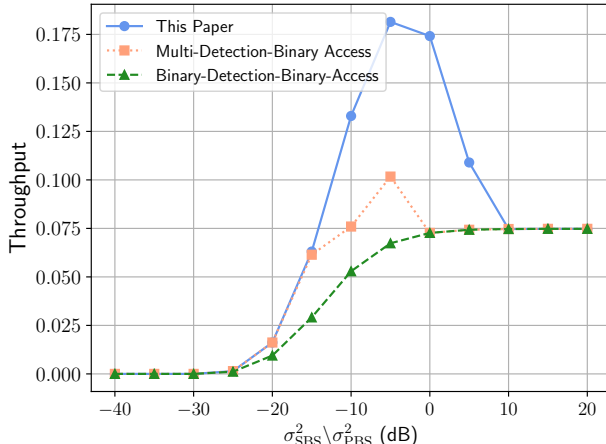


Figure 4: Throughput for the Secondary Users

Finally, we analyze the throughput of the SBS as a function of the power ratio SBS/PBS, as shown in Fig. (4). We observe that throughput increases with SBS power up to  $-5$  dB. At low power levels, the SBS transmits frequently but covers only a small portion of its intended area (assuming the SBS cell size equals that of the PBS). In this regime, our strategy always allows transmission in all directions, effectively reducing to the *Multi-Detection Binary Access* method. Between  $-10$  dB and  $-5$  dB, however, our method can exploit diverse beam combinations not used by the baselines, achieving higher throughput. Beyond  $-5$  dB, interference becomes significant, limiting SBS activity. At this point, the SBS must wait for complete PBS silence, causing all methods to converge to the *Binary-Detection Binary Access* strategy. Thus, careful tuning of SBS power is essential to maximize throughput while keeping catastrophic interference within acceptable limits. Further improvements can be achieved through the use of adaptive power control, which will be investigated in future work.

## VI. CONCLUSION

We considered a realistic infrastructure-based system with multi-beam antennas at both primary and secondary base stations. We determined the set of beams from the secondary base station that allowed secondary transmissions into different beam directions without creating excess interference for the PUs in the environment. We leveraged and showed the results for different power levels of the SBS. Our findings underscore the potential of carefully optimized multi-beam configurations to enhance coexistence and efficiency in shared spectrum.

In our future work, we will pursue the following directions: (i) relax the offline assumption of perfect channel statistics and replace it by robust estimation under partial observations; (ii) incorporate per-beam power control at both primary and secondary base stations; (iii) enhance scalability with low-complexity heuristics that offer provable approximation and regret guarantees; (iv) evaluate robustness to sensing errors,

mobility, and noise-induced channel-estimation errors using stochastic constraints and reliability analyses; (v) exploit temporal correlation in beam activity to improve low-SNR detection; and (vi) develop ML-based SINR predictors to reduce data-collection overhead.

## ACKNOWLEDGEMENT

The authors greatly appreciate the constructive discussions with Dr. Naveed Ahmed Abbasi. The work was financially supported by NSF Grant 2229535.

## REFERENCES

- [1] “Fcc, citizens broadband radio service rules.” [Online]. Available: <https://www.ecfr.gov/current/title-47/chapter-I/subchapter-D/part-96>
- [2] E. Biglieri, *Principles of cognitive radio*. Cambridge Univ. Press, 2013.
- [3] P. Setoodeh and S. Haykin, *Fundamentals of cognitive radio*. John Wiley & Sons, 2017.
- [4] A. F. Molisch, *Wireless communications, 3rd ed.: from fundamentals to beyond 5G*. IEEE Press - John Wiley & Sons, 2023.
- [5] E. Dahlman, S. Parkvall, and J. Skold, *5G NR: The next generation wireless access technology*, 1st ed. Academic Press, 2020.
- [6] D. Čabrić and M. Erić, “Spatio-temporal spectrum sensing using distributed antenna systems and direct localization methods,” in *Proceedings of the 2012 IEEE ISAP*, 2012, pp. 1–2.
- [7] N. Kleber, M. Haenggi, J. D. Chisum, B. Hochwald, and J. N. Laneman, “Directive in rf sensor networks for widespread spectrum monitoring,” *IEEE Tr. Cognitive Comm. and Networking*, vol. 8, pp. 778–792, 2021.
- [8] Y. Shi, Y. E. Sagduyu, and T. Erpek, “Federated learning for distributed spectrum sensing in nextg communication networks,” in *AI and ML for Multi-Domain Operations App. IV*, vol. 12113. SPIE, 2022, p. 12113L.
- [9] W. Na, J. Yoon, S. Cho, D. Griffith, and N. Golmie, “Centralized cooperative directional spectrum sensing for cognitive radio networks,” *IEEE Tr. Mobile Computing*, vol. 17, no. 6, pp. 1260–1274, 2018.
- [10] T. V. Nguyen and F. Baccelli, “A stochastic geometry model for cognitive radio networks,” *The Computer Journal*, vol. 55, pp. 534–552, 2012.
- [11] S. Tripathi, A. K. Gupta, and S. Amuru, “On the coverage of cognitive mmwave networks with directional sensing and communication,” *IEEE Tr. Wireless Comm.*, vol. 23, no. 10, pp. 14 215–14 231, 2024.
- [12] H. Yazdani and A. Vosoughi, “On the spectrum sensing, beam selection and power allocation in cognitive radio networks using reconfigurable antennas,” in *2019 53rd CISS*, 2019, pp. 1–7.
- [13] M. Ghaderibaneh, C. Zhan, and H. Gupta, “Deepalloc: Deep learning approach to spectrum allocation in shared spectrum systems,” *IEEE Access*, vol. 12, pp. 8432–8448, 2024.
- [14] O. P. Awe, A. Deligiannis, and S. Lambotharan, “Spatio-temporal spectrum sensing in cognitive radio networks using beamformer-aided svm algorithms,” *IEEE Access*, vol. 6, pp. 25 377–25 388, 2018.